Mathematics Today Vol.34(A) (April 2018 – Special Issue) 1-6
ISSN 0976-3228, e-ISSN 2455-9601

Designing of a mathematical model & synthesis of a fluorescent sensor which can selectively bind with drug for targeted delivery using magnetic field

Ajay L. Desai[1], Vishal Pillai[2] and Keyur D. Bhatt[1]

[1]Department of Chemistry, Mehsana Urban Institute of Sciences, Ganapat University, Kherva-384012, Gujarat, India

[2]Department of Physics, Mehsana Urban Institute of Sciences, Ganapat University, Kherva-384012, Gujarat, India

Abstract

A mathematical model for targeted drug delivery using magnetic field can be developed.A simple network model which can describe the deposition of magnetic particles in a hierarchy of vessels can be designed and the orientation of the vessels with respect to the magnetic force & its effects can be observed. In addition to fluorescence sensor, it can be targeted by binding it with drug material to study which part is affected by drug material i.e when it will bind it will fluoresce the area depending on the concentration of drug material. The life time of drug within body can also be found out with help of it.

Keywords: Mathematical Model, Drug delivery, Magnetic field and Fluorescence.

AMS Subject Classification: 92E

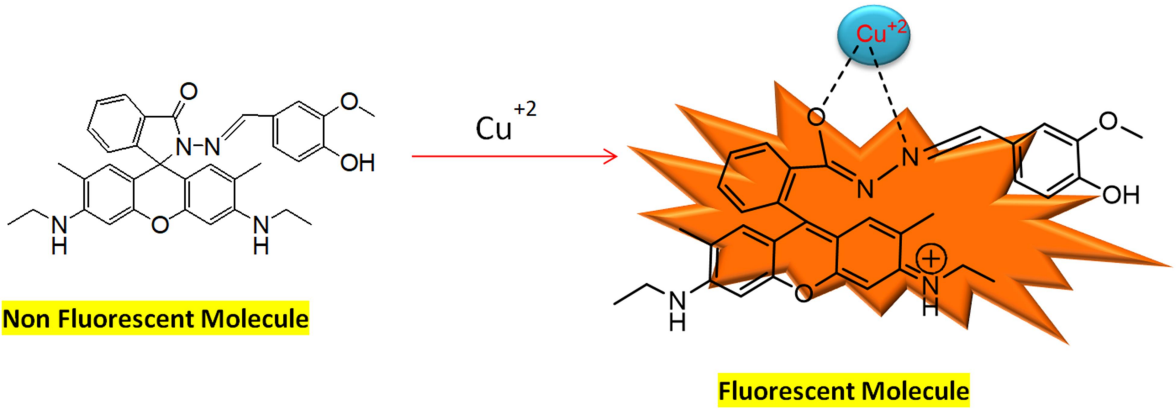

1. Introduction

In conventional drug delivery (1-3) the drug is administered by intravenous injection; it then travels to the heart from where it is pumped to all regions of the body. Where the drug is aimed at a small target region this method is extremely inefficient and leads to much larger doses (often of toxic drugs) being used than necessary (4-6). In order to overcome this problem a number of targeted drug delivery methods have been developed. One of these, magnetically targeted drug delivery, involves binding a drug to small biocompatible magnetic particles(7-9) (diameters $5*10^{-6}$ m), injecting these into the blood stream and using a high gradient magnetic field to pull them out of suspension in the target region. Once on the vessel wall the drug can either be released directly into the blood stream or a biological technique can be used to ensure uptake of the particles into the tissue. In this work we describe a theoretical analysis of this drug delivery technique(10).

Previous theoretical studies of magnetically targeted drug delivery have considered tracking individual particles under the influence of Stokes drag and a magnetic force alone. Here we also consider interactions and collisions between moving red blood cells in the bloodstream which cause a diffusive motion of the magnetic particles much greater than the standard Brownian diffusion(11). A model is formulated, suitable for studying the deposition of magnetic particles within a network of blood vessels, in the limit of low diffusivity(12). Finally, we show that it is impossible to target internal regions of the body using an externally applied magnetic field without targeting some surrounding regions more strongly. This leads us to speculate that magnetically targeted drug delivery is only suitable for target sites close to the edge of the body(13).

2. An advection–diffusion model

The motion of magnetic particles in the blood stream is modelled as an advection–diffusion process for the particle concentration c(x,t). The particle velocity v_p in the blood stream is found by balancing hydrodynamic and magnetic forces. For a particle with hydrodynamic radius a in a fluid flow, velocity v_b, Stokes drag law gives

$$v_p = v_b + v_{mag} \qquad \text{Where } v_{mag} = \frac{F_{mag}}{6\pi\mu a} \qquad (1)$$

where m is the dynamic viscosity of the fluid, and F_{mag} is the magnetic force on the particle. The Stokes drag coefficient must be modified when the particle is of the order of a few particle diameters from a solid boundary.

For small particles, Brownian motion may also be significant. This can be accounted for by introducing a particle diffusivity using the Einstein relation,

$$D_{Br} = \frac{kT}{6\pi\mu a}$$

Here T is the absolute temperature (measured in Kelvin)and k is Boltzmann's constant. A second diffusive mechanism that influences the particle motion in vessels larger than capillaries is 'shear induced diffusion'. Blood is a highly concentrated suspension of red blood cells suspended in plasma and when sheared cell—cell collisions give rise to random motions with a diffusive character. This in turn drives a diffusive motion of the

plasma, causing plasma borne particles and solutes to experience shear-induced diffusion. Measurements of the shear-induced diffusion coefficient of the plasma borne particles are difficult to obtain, however the scaling

$$D_{sh} = \dot{K_{sh}}(r_{RBC})^2\dot{\Upsilon}$$

is quite well established. Here r_{RBC} is the blood cell radius and g_ is the local value of the fluid shear rate, defined in terms of the strain rate tensor e_{ij} by the formula

$$\dot{\Upsilon} = (2e_{ij}e_{ij})^{\frac{1}{2}} = (\frac{1}{2}(\frac{\partial u_i}{\partial x_j} + \frac{\partial u_j}{\partial x_i})(\frac{\partial u_i}{\partial x_j} + \frac{\partial u_j}{\partial x_i}))^{\frac{1}{2}}$$

Where K_{sh} a dimensionless coefficient that dependson the blood cell concentration. Experimentalestimates of K_{sh} for red blood cells at physiological hematocrits showa high degree of scatter, but avalue of K_{shis} representative. Notethat the shear augmented diffusion coefficient isindependent of the particle dimensions, so that D_{sh}will take the same value for a 10 nm particle and1 mm microsphere. Theoverall diffusion coefficient is given by the sum ofthe Brownian diffusivity and the shear-induceddiffusivity, leading to a diffusive flux

$$J_{diff} = -D\nabla c \qquad \text{where} \quad D = \dot{K_{sh}}(r_{RBC})^2\dot{\Upsilon} + \frac{kT}{6\pi\mu a} \tag{2}$$

Combining the advective flux, $J_{advect} = cv_p$; and the diffusive flux contributions, and using conservation of mass, leads to an advection–diffusion equation for the particle concentration c,

$$\frac{\partial c}{\partial t} + \nabla * (cv_p) = \nabla * (D\nabla c) \tag{3}$$

The model is closed (when D<0) by imposing boundary conditions on c. These can be derived by relating the flux of particles onto the boundary of the blood vessels to the evolution of the surface density of particles on the vessel wall,

$$\frac{\partial c}{\partial t} = \boldsymbol{n} * [\boldsymbol{J}_{advect} + \boldsymbol{J}_{diff}] \mid_{boundary}$$

$$= \boldsymbol{n} * [c\boldsymbol{v}_{advect} + D\nabla c] \mid_{boundary} \tag{4}$$

(n is the outward unit normal vector at the boundary, v_b=0 at the boundary) and modeling the evolution of s by taking the particle adhesion rate to be proportional to c(x,t) at the wall, and the particle detachment rate to be proportional to s

$$\frac{\partial \sigma}{\partial t} = k_a c \mid_{boundary} - k_d \sigma \tag{5}$$

The particle adhesion and detachment rate coefficients, k_a and k_d, are functions of the particle radius, the shear rate at the wall, as well as the surface chemistry of the particle and vessel walls. The particle adhesion coefficient k_a is a decreasing functions of particle size and shear rate and that the particle detachment coefficient k_d is highest for large particles and high shear rates.

3. The magnetic field and force

The force F_{mag} and torque T_{mag} on a particle in a magnetic field B(x) are described by the formulae

$$\boldsymbol{F}_{mag} = (\boldsymbol{m} * \nabla)\boldsymbol{B} \text{ And } \boldsymbol{T}_{mag} = \boldsymbol{m} \times \boldsymbol{B}$$

Respectively, where m is the magnetic moment of the particle. Particles containing cores of magnetite material over 30 nm in diameter generally have a permanent magnetic moment. The torque T_{mag} causes such particles to rapidly align with the magnetic field so that the force F^{m}_{mag} on a permanently magnetized particle becomes

$$\boldsymbol{F}^{m}_{mag} = \frac{|\boldsymbol{m}|}{|\boldsymbol{B}|}(\boldsymbol{B} * \nabla)\boldsymbol{B} \tag{6}$$

However magnetite particles of diameter smaller than 30 nm are generally super paramagnetic. In this case m depends on the local magnetic flux density B and it is common to use a Langevin function to relate m to B,

$$\boldsymbol{m} = \frac{\boldsymbol{m}_{sat}}{|\boldsymbol{B}|}\boldsymbol{L}(|\ \boldsymbol{B}\ |)\ ,\ \boldsymbol{L}\ |\ \boldsymbol{B}\ |= \coth(\varepsilon\ |\ \boldsymbol{B}\ |) - \frac{1}{\varepsilon|\boldsymbol{B}|} \qquad \varepsilon = \frac{m_{sat}}{kT}$$

Wherem_{sat} is the saturation magnetization of the magnetic particle. Thus the force on a super paramagnetic particle is

$$\boldsymbol{F}^{m}_{mag} = m_{sat}L(|\ \boldsymbol{B}\ |)\ |\ \boldsymbol{B}\ |^{-1}\ (\boldsymbol{B} * \boldsymbol{\nabla})\boldsymbol{B}$$

For sufficiently weak fields L(|B|) can be linearized and F^{s}_{mag} approximated by

$$\boldsymbol{F}^{m}_{mag} \approx \left(\frac{\varepsilon m_{sat}}{3}\right)(\boldsymbol{B} * \boldsymbol{\nabla})\boldsymbol{B} = \frac{1}{6}\varepsilon m_{sat}\nabla(|\ \boldsymbol{B}\ |^{2}) \tag{7}$$

Magnetic field varies over a length scale determined by the magnet size typically $O(10^{-2}–10^{-1}$ m).Typical diameters of the blood vessels in whichtargeting takes place are much smaller than thisand thus magnetic force across a vessel diameter isapproximately constant.

4. Concept of Fluorescence

Additionally part of body which is influenced by drug material can also be detected successfully by designing & synthesis of a fluorescent molecule which can selectively bind with this drug material (14-16). Fluorescent sensors consists of a fluorophore (fluorescent molecule) covalently linked to an ionophore (e.g. crown ether) and is thus called a fluoro-ionophore which selectively bind alkali, alkaline and transition metal ions. The ionophore is required for selective binding of the substrate, while the fluorophore provides the means of signaling this binding, whether by fluorescence enhancement or quenching(17-19).The signalling moiety acts as a signal transducer, i.e. it converts the information (recognition event) into an optical signal expressed as the changes in the photophysical characteristics of the fluorophore(20, 21) .These changes are due to the perturbation (by the bound cation) of photoinduced processes such as electron transfer, charge transfer, energy transfer, excimer or exciplex formation or disappearance, etc.

Das et al. described a rhodamine 6G based chemosensor for the detection of Hg^{2+} and Cu^{2+}. In water-methanol (1:1, v/v) solution at pH 7.0, both Hg^{2+} and Cu^{2+} impart colour changes with new absorption peaks appearing at 534 nm for Hg^{2+} and 528 nm for Cu^{2+} [22]. A 90-fold increase in fluorescence intensity at 554 nm was

paragmatic in nature with the adding of only 8 equivalents of Hg^{2+}, while fluorescence intensity was increased due to the quenching effect of paramagnetic copper ions.

Conclusion

We have formulated a model of magnetic particle transport in the intermediate sized vessels of the blood stream which incorporates the effects of shear-induced diffusion (which arises as a result of interactions between red blood cells). The model depends crucially on the dimensionless parameter S, (see Eq. (9)). In particular if S51 the effects of the magnetic force are negligible in comparison to those of shear-induced diffusion. Estimates for magnetic particles of diameter $1X10^{-6}$–$4X10^{-6}$ m containing magnetite nano-particles (10% by volume) confirm that the diffusive flux may significantly disrupt particle deposition in arterioles and venules.We have demonstrated a simple network model which can describe the deposition of magnetic particles in a hierarchy of vessels and observed that the orientation of the vessels with respect to the magnetic force crucially affects particle depositions rates leading to heterogeneous particle distributions. In addition we have shown that it is not possible to obtain a maximum of magnetic force (on a magnetic particle) inside the body, using an externally applied magnetic field. Since drug targeting is effected by pulling magnetic particles to the edge of vessels this suggests that it will not be possible to target interior regions of the body without targeting some of the surrounding regions of the body more strongly. Furthermore we do not expect magnetic traps to be of use in this application since magnetic particles are constrained to move around the body in linear vessels and the magnitude of magnetic field required to hold a particle in the main flow, of all but the very smallest of vessels, is very large. This leads us to conjecture that the use of magnetically targeted drug delivery with an externally applied field is appropriate only for targets close to the surface of the body.

Acknowledgment:

The authors gratefully acknowledge the Instruments and software facility provided by Ganpat University. The authors also acknowledge GUJCOST, Gandhinagar, Gujarat University, Ahmedabad and Centre of excellence (Rajkot) and INFLIBNET (Ahmedabad) for e-journals.

References:

1. LIU, J., BU, W., PAN, L. & SHI, J. (2013) NIR-Triggered Anticancer Drug Delivery by Upconverting Nanoparticles with Integrated Azobenzene-Modified Mesoporous Silica, *Angewandte Chemie International Edition*, 52, 4375-4379.
2. LU, J., LIONG, M., LI, Z., ZINK, J. I. & TAMANOI, F. (2010) Biocompatibility, biodistribution, and drug-delivery efficiency of mesoporous silica nanoparticles for cancer therapy in animals, *Small*, 6, 1794-1805.
3. VALLET-REGÍ, M., BALAS, F. & ARCOS, D. (2007) Mesoporous materials for drug delivery, *Angewandte Chemie International Edition*, 46, 7548-7558.
4. BAE, Y., FUKUSHIMA, S., HARADA, A. & KATAOKA, K. (2003) Design of environment-sensitive supramolecular assemblies for intracellular drug delivery: Polymeric micelles that are responsive to intracellular pH change, *Angewandte Chemie International Edition*, 42, 4640-4643.

5. CHAN, D. C., CHUTKOWSKI, C. T. & KIM, P. S. (1998) Evidence that a prominent cavity in the coiled coil of HIV type 1 gp41 is an attractive drug target, *Proceedings of the National Academy of Sciences*, 95, 15613-15617.
6. ZHANG, B. B., ZHOU, G. & LI, C. (2009) AMPK: an emerging drug target for diabetes and the metabolic syndrome, *Cell metabolism*, 9, 407-416.
7. ALBORNOZ, C. & JACOBO, S. E. (2006) Preparation of a biocompatible magnetic film from an aqueous ferrofluid, *Journal of magnetism and magnetic materials*, 305, 12-15.
8. GOETZE, T., GANSAU, C., BUSKE, N. et al. (2002) Biocompatible magnetic core/shell nanoparticles, *Journal of Magnetism and Magnetic Materials*, 252, 399-402.
9. MAHDAVI, M., AHMAD, M. B., HARON, M. J. et al. (2013) Synthesis, surface modification and characterisation of biocompatible magnetic iron oxide nanoparticles for biomedical applications, *Molecules*, 18, 7533-7548.
10. HORCAJADA, P., SERRE, C., VALLET-REGÍ, M. et al. (2006) Metal–organic frameworks as efficient materials for drug delivery, *Angewandte chemie*, 118, 6120-6124.
11. RITCHIE, K., SHAN, X.-Y., KONDO, J. et al. (2005) Detection of non-Brownian diffusion in the cell membrane in single molecule tracking, *Biophysical journal*, 88, 2266-2277.
12. GOODWIN, S., PETERSON, C., HOH, C. & BITTNER, C. (1999) Targeting and retention of magnetic targeted carriers (MTCs) enhancing intra-arterial chemotherapy, *Journal of Magnetism and Magnetic Materials*, 194, 132-139.
13. BATCHELOR, G. (1976) Brownian diffusion of particles with hydrodynamic interaction, *Journal of Fluid Mechanics*, 74, 1-29.
14. HIRATA, S., SAKAI, Y., MASUI, K. et al. (2015) Highly efficient blue electroluminescence based on thermally activated delayed fluorescence, *Nature materials*, 14, 330-336.
15. LEE, M. H., KIM, J. S. & SESSLER, J. L. (2015) Small molecule-based ratiometric fluorescence probes for cations, anions, and biomolecules, *Chemical Society Reviews*, 44, 4185-4191.
16. WEGNER, K. D. & HILDEBRANDT, N. (2015) Quantum dots: bright and versatile in vitro and in vivo fluorescence imaging biosensors, *Chemical Society Reviews*, 44, 4792-4834.
17. BHATT, K. D., GUPTE, H. S., MAKWANA, B. A. et al. (2012) Calix receptor edifice; scrupulous turn off fluorescent sensor for Fe (III), Co (II) and Cu (II), *Journal of fluorescence*, 22, 1493-1500.
18. BHATT, K. D., SHAH, H. D. & PANCHAL, M. (2017) A switch-off fluorescence probe towards Pb (II) and cu (II) ions based on a calix [4] pyrrole bearing amino-quinoline group, *Luminescence*.
19. MAKWANA, B. A., VYAS, D. J., BHATT, K. D., JAIN, V. K. & AGRAWAL, Y. K. (2015) Highly stable antibacterial silver nanoparticles as selective fluorescent sensor for Fe 3+ ions, *Spectrochimica Acta Part A: Molecular and Biomolecular Spectroscopy*, 134, 73-80.
20. BORICHA, V. P., PATRA, S., PARIHAR, S., CHOUHAN, Y. S. & PAUL, P. (2012) Luminescent metalloreceptors with pendant macrocyclic ionophores with NS 2 O 3 donor sites: Synthesis, characterization and ion-binding property, *Polyhedron*, 43, 104-113.
21. PARIHAR, S., BORICHA, V. P. & JADEJA, R. (2015) Pyrazolone as a recognition site: Rhodamine 6G-based fluorescent probe for the selective recognition of Fe3+ in acetonitrile–aqueous solution, *Luminescence*, 30, 168-174.